Acc. Chem. Res. **1998,** *31,* 257−266

Studies of Potential Generation Across Membrane Sensors at Interfaces and through Bulk

RICHARD P. BUCK*,† AND ERNO LINDNER‡

Department of Chemistry, University of North Carolina, Chapel Hill, North Carolina 27599-3290, and Department of Biomedical Engineering, Duke University, Durham, North Carolina 27708-0295

Received May 7, 1997

Introduction

Modern potentiometric and amperometric sensors for measuring and monitoring ion activities and neutral species concentrations are passive membrane-based systems. The ion-sensing membranes described in this Account contain charged species and are ion exchangers. They are polyelectrolytes or equivalent plasticized polymer/hydrophobic salt mixtures, which are different from the passive membranes used in SAW (surface acoustic wave) devices. Our membranes are related to packings used in ion chromatography, while SAW membranes are analogous to HPLC packings. Our membranes generate voltages and control currents passing through them. They revolutionized analytical chemistry through their superb selectivity and sensitivity, and made possible simple, separation-free, continuous monitoring. They can be made by photolithographic microfabrication in extremely small sizes to analyze samples of submicroliter volume. Microelectrochemical sensors are used for probing single cells, can follow ionic transients in the ischemic heart, and can serve as detectors in liquid chromatography.

Discovery and development have occurred simultaneously with increased appreciation of the origins of potential generation and current control. To understand the development of measured signals, potential difference (pd) between the two sides of the membrane at open circuit (potentiometry) and current arising from applied voltages across membranes (amperometry), a simple set of concepts and design principles have arisen. Energy imbalances at interfaces lead to unbalanced charge (space charge), electric fields, and measured pds through the interface regions. Processes of potential difference development depend on the competitive energetics of the interactions between ions and solvent and complex-forming species in each phase: bathing electrolyte and membrane. In bulk phases, the creation of an internal electric field arises from the separation of fast and slow moving ions, while fulfilling the requirement of bulk electroneutrality during charge transport. Three potential components contribute to the measured signal: the two interfacial pds (determined by electronic and ionic charge exchange processes) and the interior, bulk pd (determined by charge motion via diffusion and migration).

Classical Galvanic cells, with or without liquid junctions, did not include membranes or phases with variable compositions.[1] The cell

$$\mathrm{Ag/AgCl/Cl^-||MX(aqueous)|membrane|NX\ (aqueous)||Cl^-/AgCl/Ag}$$

reaches steady state as solutions slowly flow through the membrane. For a hydrophilic site free membrane such as cellophane, MX and NX transfer in a counterflow manner. For a permselective negative-site membrane, M^+ moves from left to right and N^+ moves in the reverse direction. For a positive-site membrane there is no anion transport at zero current for the cell as shown. However, if the right compartment contained NY, then Y^- would move to the left compartment, while X^- moves to the right. These cells represent typical situations of zero current, but nonzero fluxes. Simulations demonstrate these effects.[2,3] Cartoons of a cation-exchange membrane, exposed to bathing solutions of M^+ and N^+ in symmetric and asymmetric cell arrangements, are given in Figure 1.

The potential profile runs continuously from the contacting phase on one side, through the membrane, to the contacting phase on the other side. Processes that generate and modify the membrane's electrical features include ion exchange, complex formation, and transport. The important features of membranes used in electrochemical cells are controlled by the potential profiles, space charge densities, and concentration profiles. In this paper experimental results by various techniques are summarized on (1) quasi-absolute interfacial pds by convention, (2) distribution of pds and space charge in each contacting immiscible phase, (3) transport of charge through the interfaces, (4) slow interfacial ion transfer kinetics, (5) bulk transport, (6) membrane impedances, and (7) chronoamperometric studies of interior pds and concentrations during transport. Experimental data confirm the energy-based criteria for pd generation, and give researchers and users confidence when predicting important parameters that must be controlled or modified to achieve selective responses of sensors. Since potentiometric and amperometric responses are connected by the $i-\phi$ (current−voltage) characteristic of a cell, there are no new concepts required to interpret responses of cells with various contact types: ion exchange or electron exchange. Thus,

Richard P. Buck received his B.S. from the California Institute of Technology in 1950, his M.S. in 1951, and his Ph.D. from MIT in 1955. After many years in industry, he joined the Faculty of the University of North Carolina at Chapel Hill in 1967 and has been Professor since 1975. His interests include transport of charged species in solids and liquids, in bulk, and across interfaces and applications of films and membranes in materials science and sensor technology.

Erno Lindner received his Ph.D. degree from the Technical University of Budapest. He was awarded a D.Sc. by the Hungarian Academy of Sciences, and became Full Professor in 1994. He is presently in the Department of Biomedical Engineering at Duke University pursuing research in biomedical sensors.

† University of North Carolina.
‡ Duke University.

S0001-4842(97)00062-9 CCC: $15.00
Published on Web 05/02/1998

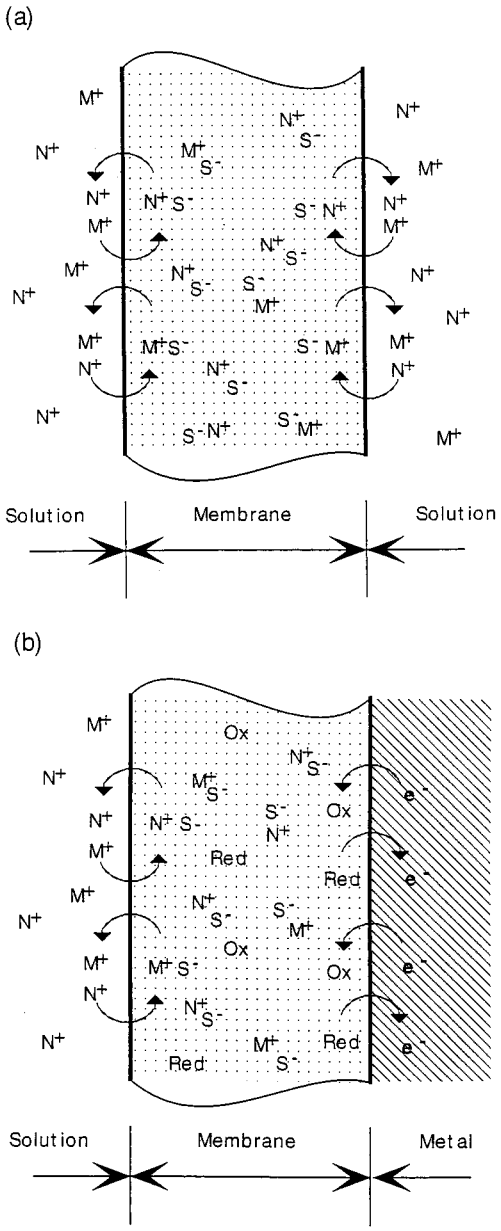

FIGURE 1. (a) A symmetrically bathed membrane containing negatively charged sites (mobile or fixed sites, S^-) exposed to bathing solutions of counterions M^+ and N^+. (b) An asymmetrical contacted membrane containing negatively charged sites (mobile or fixed sites, S^-) and a cationic redox couple, exposed to inert metal and to a bathing solution of counterions M^+ and N^+. The membrane is electroneutral. The negatively charged sites are balanced by the total charge of Ox, Red, M^+, and N^+. Normally concentrations of Ox and Red $\ll$ M^+ and N^+

we introduce concepts of symmetric and asymmetric sensor cells. Potentiometric responses are emphasized.

Segmented Potential Difference Model of Teorell–Meyer–Sievers (TMS). Mentally splitting the continuous potential profile across a membrane into three segments is an old idea. In 1936, Teorell[4,5] and Meyer and Sievers[6] recognized that evaluation of the whole membrane pd was the difficult point in calculating the cell voltage. They split the membrane pd into two interfacial pds and the interior bulk diffusion pd.

$$\Delta\phi = \phi_{\text{right}} - \phi_{\text{left}} = [\phi(\text{right soln}) - \phi(\text{memb right interface})] + [\phi(\text{memb right interface}) - \phi(\text{memb left interface})] + [\phi(\text{memb left interface}) - \phi(\text{left soln})]$$

This quantity is the net membrane pd, e.g., the "inner" potential of the right-hand solution less the potential of the left-hand solution. Assuming linear ion concentration profiles, integration of the electric field in terms of the combined ion profiles gave a closed form for the interior bulk membrane pd. Then, the Nernst–Donnan equation was applied to each equilibrium ion exchange or extraction process to compute the interfacial pds.[7] TMS distribution of potential is illustrated diagramatically in Figure 2.

In more general treatments of the bulk pds,[8] the differential diffusion pd is integrated or expressed as an integral, and the interfacial pds are added. The result is the same as TMS theory when ion profiles are linear. In more general cases different results are obtained. Examples of membrane transport analysis, with determination of species with linear concentration profiles, are treated in studies on experimental conditions when Donnan exclusion failure (loss of permselective transport) deteriorates the Nernstian responses of liquid ion exchanger membranes.[9–12]

Building Specific Permselectivity into Ion Exchanger Membranes. The preference of the membranes for M^+ or N^+ is not defined in Figure 1. However, the ion exchange equilibrium constant and free energy of exchange of M^+ and N^+ are thermodynamic quantities that can be determined. One can mentally subdivide these quantities into two nonthermodynamic quantities: the single-ion partition coefficients and single-ion free energies of transfer. For water-swollen ion exchangers and solvent-plasticized ion exchanger membranes, there are empirical series of salts with a common cation that show increasing stability of anions in positive-site anion-exchanging membranes. Likewise, there are series of salts with a common anion with gradually changing cation stabilities in cation exchangers. These are Hofmeister lyotropic series. The elementary interpretation is based on electrostatic factors that account for ion charge and size and membrane dielectric constant (see ref 8, Chapter 5 pp 151–200). The Born equation is used for calculating the transfer energy.

The selectivity series can be modified through changes of the membrane dielectric properties, e.g., by using different plasticizers or by compounding membranes with selective hydrophobic complexing agents: neutral or charged carriers. Addition of carriers (ionophores) into the membrane phase, Figure 3, confers special selectivity to the counterion exchange or extraction processes that forces a non-Hofmeister response.[13–16] The ion exchange or partitioning of a desired counterion is accompanied by formation of an association complex. For uncharged carriers, the bonding is of ion–dipole interaction type, and characteristic structures, typically octahedral, of carbonyl and ether oxygens of the carriers are involved. In the

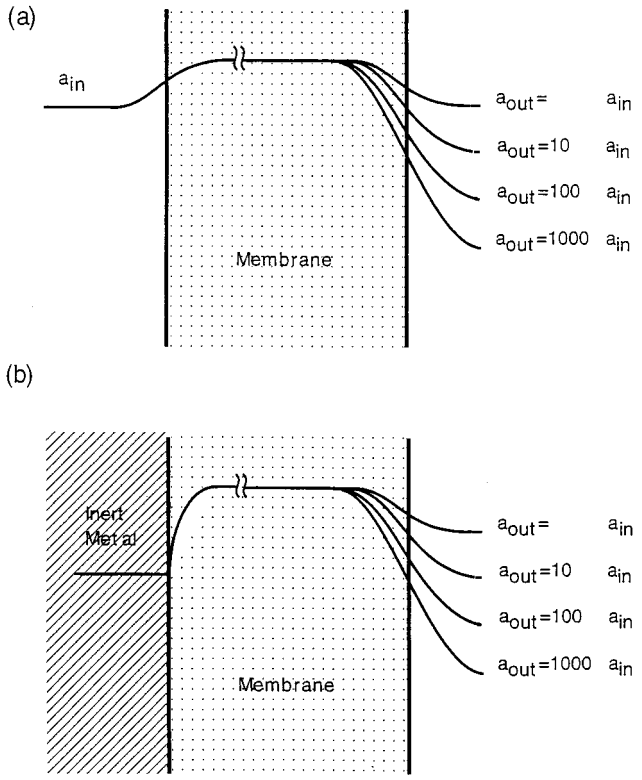

FIGURE 2. (a) Schematic potential profile for a membrane containing exchangeable cations with either (1) a lower cation concentration in the membrane than in either bathing solution or (2) a very favorable ion extraction coefficient k_i. (b) Schematic potential profile for a membrane containing exchangeable cations and a cationic redox couple that exchanges e^- with the inert metal. The potential profiles correspond with positive space charge in the membrane; i.e., metal is negative.

mechanism of ion exchange, the carrier at the surface gradually dehydrates and binds the hydrated ion to form an oil-soluble ion−carrier complex. There is very little aqueous phase carrier or ion−carrier complex. On the other hand, metalloporphyrins and other metalloalkyl salts (e.g., alkyltin dichlorides) can induce anion-selective responses. These carriers appear to form weak metal−anion adducts.

Ion Exchange and Carrier Membranes Contrasted. Plasticized polymer membranes, such as poly(vinyl chloride) (PVC) and dioctyl sebacate (1:2 wt ratio), serve as a basic starting material. They are nonselective, low-site-density cation exchangers and are permselective over a limited bathing solution composition. The natural negative-site concentration of PVC membranes is about 0.05−1 mM and thought to be mainly carboxylate.[17] Properties of ionophore-loaded membranes are influenced by the kind (mobile or fixed) and concentration of sites. To control membrane properties, we do not rely on the presence of impurity sites in commercial polymers. Instead, tetraphenylborate salts or their derivatives, added at the 10 mM level to the membrane, are trapped by hydrophobic interactions. The mole ratio of carrier to site concentration is adjusted to be optimal for counterion−carrier complex stoichiometry. For univalent cations and

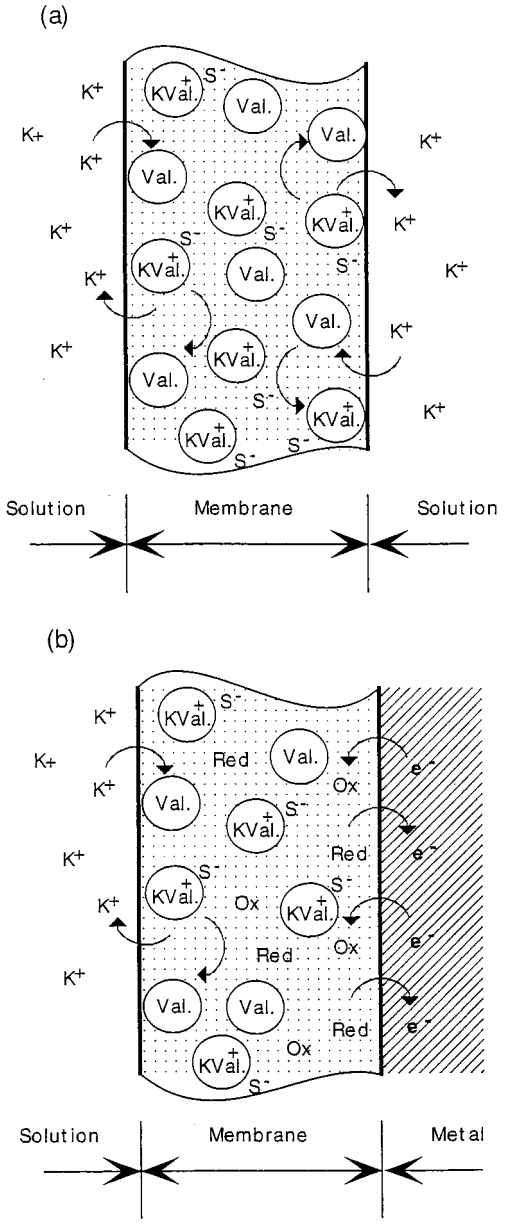

FIGURE 3. (a, b) As in 1a,b, but the membrane contains a lipophilic complexing agent (neutral carrier) for K^+, typically valinomycin (Val) so that only one counterion species, K^+ is extracted into the membrane.

1:1 stoichiometry, the mole ratio must exceed unity. A 2:1 ratio with excess free carrier is thought to be ideal.[18]

In potentiometric sensors, selective ion exchange and mobility of the ion−carrier complex are crucial. These properties are necessary to create the inner potential or field profile throughout the membrane. Once the ion−carrier complex is formed in the membrane by interfacial ion exchange and bulk diffusion, there is no further need for "carrying". A step concentration of selected ion, say K^+, at a membrane/electrolyte interface, does not require extensive motion of free carrier, ion−carrier complex, or sites within the membrane. Only the space charge in the back-to-back double layers is reshuffled slightly to generate the larger (or smaller) interfacial pd at that one interface. These profiles are illustrated in Figure 2.[16]

Table 1. Cells with Symmetric and Asymmetric Contacts

Symmetric Ionic/Ionic Contact Cells	
$Ag/AgCl/Cl^-\|\|MX$ (aqueous)|membrane|MX(aqueous)|| $Cl^-/AgCl/Ag$	(I)
Asymmetric Ionic/Electronic Contact Cells	
$Ag/AgCl/Cl^-\|\|MX$(aqueous)|membrane|inert metal	(IIA)
Metal/Metal Ion Half-Cell, and Nonmetal/Nonmetal Ion Half-Cell Contacts	
reactive metal|membrane|reactive nonmetal	(IIB)
Symmetric Electronic Contact Cells	
inert metal|membrane|inert metal	(III)

Membrane-Based Electrodes and Cells Covered by a General TMS Model. Membranes and films used in sensors can be liquids, semisolid gels, glassy or solid systems of ion conductors, and mixed electron/ion conductors. They are organized into symmetric and asymmetric interface cells.[19] Examples are given in Table 1. Cells I and III are symmetric because the membrane is contacted with ion or electron conductors on both sides.[19−21] Cell I is used to determine ionic properties since electron transport across both interfaces is blocked, unless one specifically incorporates pairs of redox ions in all phases. Conversely, cell III isolates electronic transport since ion transfer is blocked at the interfaces.

Cells IIA and IIB are asymmetric,[19−21] and necessarily involve transport of ions through one interface and electrons through the other (IIA) or electrons crossing the interfaces in opposite directions (IIB). The permselective membranes in asymmetric cells of IIA for sensing cations or for anions, in addition to containing the cation or anion, must be low-loaded with pairs of redox ions, e.g., ferri/ferrocyanide in anion-exchanger membranes, or Ru(II/III) complex cations in cation exchanger membranes. Low-loaded means that the concentration of the redox couple is about 10 mol % of the trapped site concentration. The metal electrode can then be reversibly poised.[7] At the left interface, cations or anions exchange at equilibrium.

Other mixed conductors can be used in anion-exchanger-based sensors: (1) polymeric cation/neutral polymer redox couples; (2) insoluble cation radical salt and corresponding neutral compound, and (3) redox metal-center polymer film coatings such as an anion exchanger formed from polymeric Os(II/III) X^-.[22,23] Partly oxidized polyanilines, polypyrroles, and polyindoles form sensors that resemble radical salt anion sensor electrodes made by Sharp.[24]

Cell III can be composed of membranes with or without sites. The membrane might consist of a pair of redox counterions in a fixed-site, or a trapped, mobile-site membrane. If there were no fixed sites in the membrane, it may contain redox ions and charge-compensating counterions by extraction of whole salts from the contacting electrolyte solutions. Many examples of types I, II, and III were included in a recent book.[1]

Membrane phases may be physically inhomogeneous from bulk to surface regions, in terms of porosity and gross species concentration. Impurity segregation or separation of phases into more resistive layers occurs near the surfaces. Recent studies show inhomogeneous surface regions for solvent polymeric membranes.[15,25−31]

Theoretical Basis for Analyzing the General TMS Model. It is the energy difference of individual ionic species in the two adjacent phases that drives and controls the interfacial potential generation processes through space charge generation. Reorientation of solvent molecules, and adsorption of ions, may also contribute to the interfacial pd. The energies of charged species are partial molar free energies or electrochemical potentials. For electrons in each phase, the electrochemical potentials are the Fermi levels:

$$\tilde{\mu}_e = \epsilon + (RT/n)\ln(a_{re}/a_{ox}) - F\phi \tag{2}$$

$$n = z_{ox} - z_{re} \tag{3}$$

For electrons in metals

$$\tilde{\mu}_m = \epsilon - F\phi \tag{4}$$

For ions, the equivalent electrochemical potentials are

$$\tilde{\mu}_i = \mu_i^0 + RT\ln(a_i) + z_iF\phi \tag{5}$$

Upon equating Fermi levels, differences in "standard" energies, ϵ's, are linearly related to the negatives of the standard electrode potentials. $\tilde{\mu}$'s are energies (electrochemical potentials), R and T are the gas constant and absolute temperature, n is the number of electrons transferred between redox species ox and red, F is the Faraday constant, z_i is an ion charge, a's are activities, and ϕ is the Galvani or "inner" potential of a phase. For neutral salts in any phase, the chemical potentials are the stoichiometric sum of electrochemical potentials of constituent ions.

Interfacial Potential Differences. The electrochemical potentials of all equilibrated species, regardless of sign, have to be equated to determine the interfacial pd. The basic equation for the interfacial pd in terms of a single species is

$$\exp[(z_iF/RT)\Delta\phi] = [k_ia_i/\bar{a}_i] \tag{6}$$

The interfacial pd

$$\Delta\phi = \bar{\phi} - \phi \tag{7}$$

is found in terms of single-ion internal and external activities. The internal membrane or film quantities use a super bar. The difference of standard state free energies of the ions in each phase defines the single-ion partition coefficients k_i and the standard interfacial pd $\Delta\phi^0$. The standard free energies are extrapolated infinite dilution quantities where activity coefficients are unity in each phase.

$$z_iF\Delta\phi_i^0 = RT\ln k_i = \mu_i^0 - \bar{\mu}_i^0 \tag{8}$$

The free energy change (species standard chemical potential difference) on the right is the "medium effect", e.g., the energy or work of transfer of an infinitely dilute ion

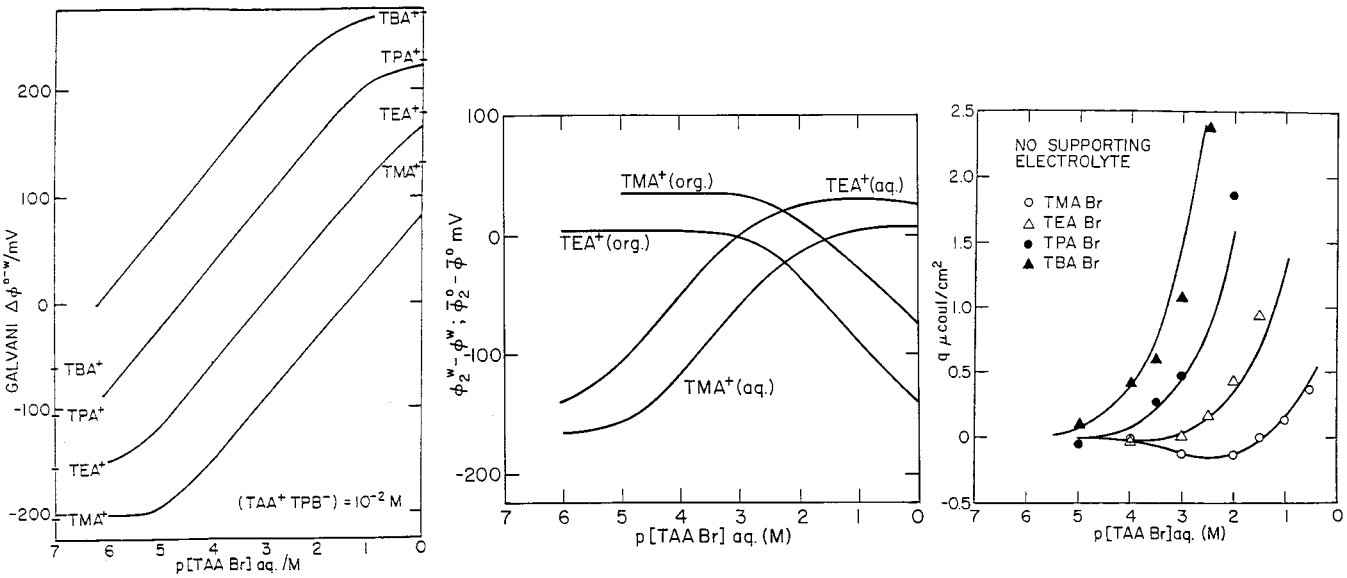

FIGURE 4. (a, left) Calculated potential differences across the nitrobenzene/water interface as a function of aqueous TAABr concentration. The corresponding TAATPB in nitrobenzene is constant at 10^{-2} M. Calculation is based on the TPAsTPB equi-energy ion extraction assumption. TAA = tetraalkylammonium and M, E, P, B = methyl, ethyl, propyl, and butyl. Reprinted with permission from ref 34. Copyright 1983 Elsevier. (b, middle) Double diffuse layer potential profiles in water and nitrobenzene from the Lippmann equation analysis of maximum bubble pressure data (surface excess charge) using the Verwey−Niessen calculation. These data allow the net pd (in (a)) to be subdivided into the portions existing in each phase that add to the total. Superscript o and w = oil and water. Reprinted with permission from ref 34. Copyright 1983 Elsevier. (c, right) Surface charge densities calculated from the Lippmann equation for the maximum bubble pressure experiment on the surface tension of the interface. These data establish the formation of space charge that determines the changing values of surface tension. The lines indicate values from the Verwey−Niessen theory. Reprinted with permission from ref 34. Copyright 1983 Elsevier.

from water to the membrane. When the membrane is a water-swollen synthetic ion exchanger, the medium effect is close to zero except for small pV terms. Then $k_i = 1$ for conventional ion-exchanger bead phases. However, the single ion partition coefficient is normally different from unity, especially for membranes containing low dielectric constant plasticizers.

Equienergetic Reference Standard: Tetraphenylarsonium Tetraphenyl-borate. Using the equations above for the extraction free energy of a salt

$$\Delta G^0_{ext} = -RT \ln K_{ext} = -RT \ln k_+k_- = (\bar{\mu}_+^0 - \mu_+^0) + (\bar{\mu}_-^0 - \mu_-^0) \quad (9)$$

For the standard partitioning substance, tetraphenylarsonium (TPAs) tetraphenylborate (TPB), an extrathermodynamic assumption is made. The two ion medium effect free energies are *assumed* equal to $\Delta G^0_{ext}/2$. This standard extraction free energy is related to the salt extraction coefficient K_{ext} and the two single-ion coefficients in (9). By measuring the interfacial pd at an immiscible liquid/liquid interface, for a series of cation TPB anion salts, free energies of single-ion transfers and standard $\Delta\phi^0$'s can be computed and compared with experiment.[32,33] This convention provides our best estimate for quasi-absolute interfacial pd components of the TMS model.

Testing the Teorell−Meyer−Sievers Theory

Equilibrium at Immiscible Liquid/Liquid Interfaces. Interfacial tension at a single membrane/bathing electrolyte interface can be measured using the maximum bubble pressure method.[34] The surface charge is computed using the Lippmann equation. If there is no linear pd from aligned dipoles, then the Gouy−Chapman theory,[35] modified by Verwey and Niessen[36] for back-to-back space charge double layers, can confirm the potential profiles in each phase whose total must be the net interfacial pd. Electrocapillary curves were constructed by varying the concentration of tetraalkylammonium bromides (from tetramethyl to tetrabutyl) in water with $TPAs^+$ TPB^- as electrolyte in the nitrobenzene immiscible phase. Typical examples of results are in Figure 4. The first direct measurement of the Verwey−Niessen back-to-back double-layer capacitance is shown in Figure 5. These measurements confirm the curvature regions between bulk and interfacial pds.

Nonequilibrium Immiscible Liquid/Liquid Interfaces: Mass Transport. New phenomena were discovered during studies of two-ion (simple salt) transport across immiscible liquid/liquid interfaces. They are called "electrosorption and electrodesorption".[37,38] When a single salt transports under an applied voltage (say reversible cation and anion in each phase, with equilibrium partitioning between phases), the salt concentration profile can be constant in each phase, the solution resistance is ohmic, and dc currents are independent of time. These results are rare exceptions that happen only when all diffusion coefficients are equal. Usually, when the coupled diffusion coefficients are unequal, salt can accumulate at the interface (electrosorption) or deplete (electrodesorption) depending on the direction of current. There are

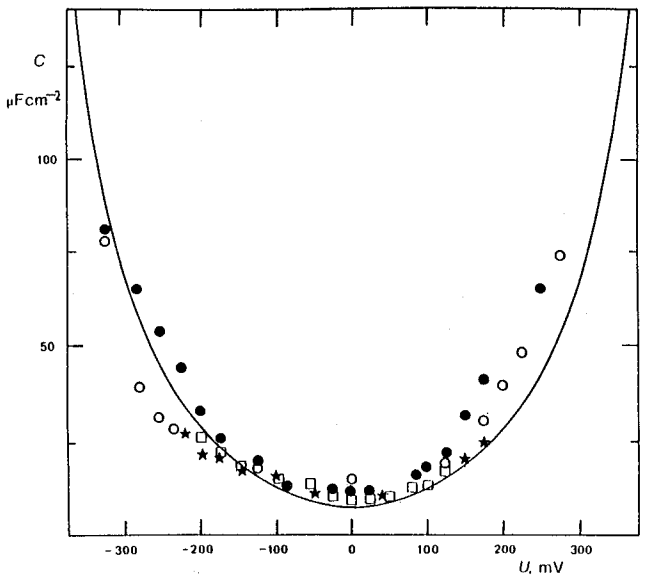

FIGURE 5. Specific capacitance of the back-to-back doubly diffuse interface water/nitrobenzene. The interface is polarizable and uses 0.01 M NaCl and 0.05 M TPAsTPB as electrolytes. Although this quantity can be obtained from the data in Figure 4, the imaginary impedance directly measures the capacitance more accurately. The interfacial pd, called U, is the $\Delta\phi^{o-w}$ of the text. Reprinted with permission from ref 64. Copyright 1984 Elsevier.

six cases: cases I and II, a single ion of ± charge is reversibly transferred from the aqueous to organic phase (or the reverse) in inert, nonpartitioning supporting electrolyte (I) or *absence* of supporting electrolyte (II); cases III and IV, two ions of opposite charge reversibly transfer through aqueous/organic interfaces in the *presence* (III) and *absence* (IV) of supporting electrolyte; case V, a single ion of charge ±1 reversibly transfers from the aqueous phase with supporting electrolyte to the organic phase without supporting electrolyte (or the reverse); case VI, two ions of charge ±1 reversibly transfer across aqueous/organic interfaces from phases with aqueous supporting electrolyte, but no organic supporting electrolyte. Some of these interesting effects are illustrated in Figure 6 (normal supported electrolyte case II) and 7 (electrosorption/desorption, case IV). These unusual two-phase mobile transport phenomena are characteristic of immiscible electrolyte chemistry and are not observed with ordinary transport to and from solid electrodes.

Slow Ionic Charge Exchange at Interfaces. Many times, the slow rate of ion transfer at one interface determines the current. Usually it is the lower concentration side of the immiscible interface. The defining (1) of the reversible TMS theory still applies, but the interfacial pds may differ from the Nernst or Nernst−Donnan values. Recent molecular dynamic simulations suggest that classical activated electron transfer models may not apply to slow ion transfer kinetics. Aqueous electrolyte/immiscible liquid ion-exchanger membrane interfaces are not molecularly flat planes. Immiscible liquid interfaces are prone to thermally generated molecular roughness. Massive restructuring of the surface includes jets of one solvent penetrating temporarily into the other phase and vice versa.[39−42]

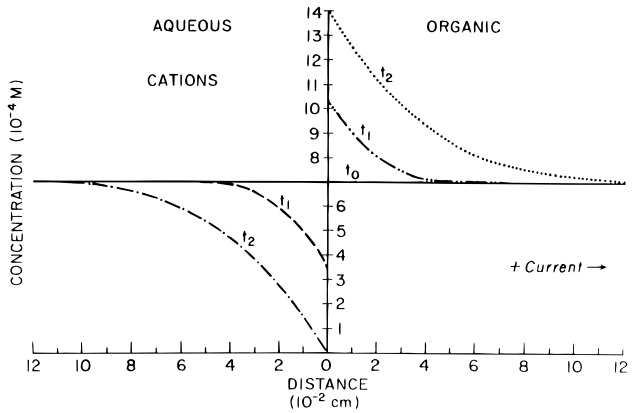

FIGURE 6. Concentration−distance−time profiles for case II: one cation (present in both phases, anions blocked) moving from left to right at two successive times, t_1 and t_2, after an initial uniform (flat) concentration profile at $t = 0$. No supporting electrolyte. Details in ref 37. Reprinted with permission from ref 37. Copyright 1981 Elsevier.

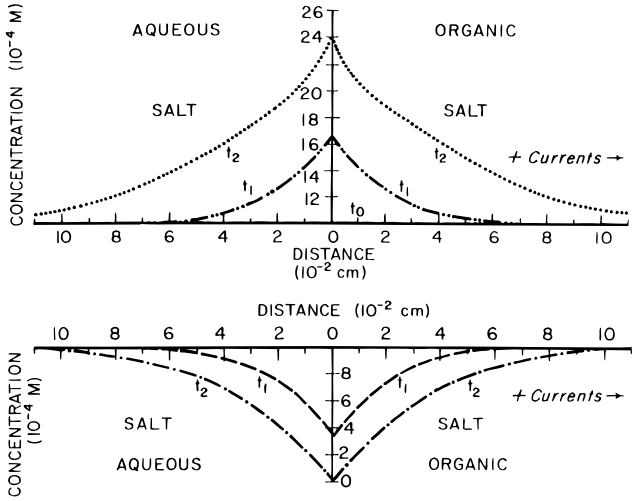

FIGURE 7. (a, top) Concentration−distance−time profiles for case IV: ***electrosorption***, univalent reversible cations and anions (one partitioned salt); aqueous cations moving to organic phase; anions moving from organic to aqueous phase; no supporting electrolyte; $K = 1$. D(aq) for the cation and D(org) for the anion are much larger than the other two D's. Details in refs. 37 and 38. Reprinted with permission from ref 37. Copyright 1981 Elsevier. (b, bottom) Concentration−distance−time profiles for case IV: ***electrodesorption***, two univalent reversible ions (one partitioned salt); aqueous cations moving to organic phase; anions moving from organic to aqueous phase; no supporting electrolyte; $K = 1$. D(org) for the cation and D(aq) for the anion are much larger than the other two D's. Details in refs 37 and 38. Reprinted with permission from ref 37. Copyright 1981 Elsevier.

In our papers, ion transfer rates have been treated as "activated" across a sharp, flat interface meniscus following the Butler−Volmer−Erdey−Gruz model, with exponential concentration variations within the perturbed back-to-back double layers.[43,44] A second, newer model based on a mixed-solvent layer barrier of constant thickness has gained advocates.[45,46] In the newer model the apparent rate constant is D/δ, the operating diffusion coefficient of the barrier region divided by its thickness.[47−50]

Processes in Bulk: Generation of Diffusion−Migration Potential Differences. Transport properties are deduced from the flux equations using macroscopic mobilities.[23,25,51−54] For electrons (e) (in the absence of band structures) and for ions (i), the fluxes J_e and J_i are

$$J_e = -u_e C_{ox} C_{re}\, \partial\tilde{\mu}_e/\partial x \qquad (10)$$

and

$$J_i = -u_i C_i\, \partial\tilde{\mu}_i/\partial x \qquad (11)$$

where u's are mobilities and $\tilde{\mu}$'s are electrochemical potentials. The continuity equation is used for time dependences. Internal bulk diffusion−migration pds are computed by rearranging and solving these equations.

The applied voltage at steady state appears as two perturbed interfacial pds and this potential drops in the bulk. Steady-state concentration profiles have been described.[55] The mathematical description of concentration profiles, internal pds, and fluxes follows a number of simple principles.[56] The important concepts include quasi-electroneutrality in bulk, flux coupling in bulk, and interfacial fluxes in terms of gradients and tranference numbers. Second-order electron hopping with ion coupling is relatively new in papers by Buck.[23,53] Digitally simulated solutions of transport equations are given for the transient and steady-state concentration profiles, fields, and potentials in bulk.[2,3,12,57]

Experimental Measurements of Mass Transport and Surface Processes

Spectropotentiometry: Imaging Methods under Electrochemical Control. Carriers for protons can be found that exhibit different colors for the free and complexed (protonated) carrier. An example is ETH 5294 (a hydrophobic derivative of Nile Blue) existing as the red free form (λ_{max} = 535 nm) and as the blue protonated form (λ_{max} = 655 nm). Four thin (approximately 50 μm) DOS (dioctyl sebacate)-plasticized poly(vinyl chloride) membranes, containing high concentrations of TPB^- and carrier were stacked and subjected to a 3 V dc voltage.[58] In this relatively weakly ion-paired system, concentration polarization of the free carrier controls the limiting current, Figure 8a, while anion concentration remains nearly uniform. At the end of the experiment each membrane shows a different concentration of free carrier. Upon reassembling the membrane stack and shorting the cell, the carrier diffuses back to nearly uniform concentration, as indicated by the right panel. This is an example of current control by *free carrier diffusion*.

By lowering the concentration of mobile-site anions and by selecting a more oil-soluble anion, tetrakis[3,5-bis(trifluoromethyl)phenyl]borate, concentration polarization of the anionic sites controls the current as illustrated in Figure 8b. The central panel represents the analysis after dc polarization, while the right panel shows results after reassembling and relaxation of the concentration profiles. This is an example of control by trapped *site diffusion*.

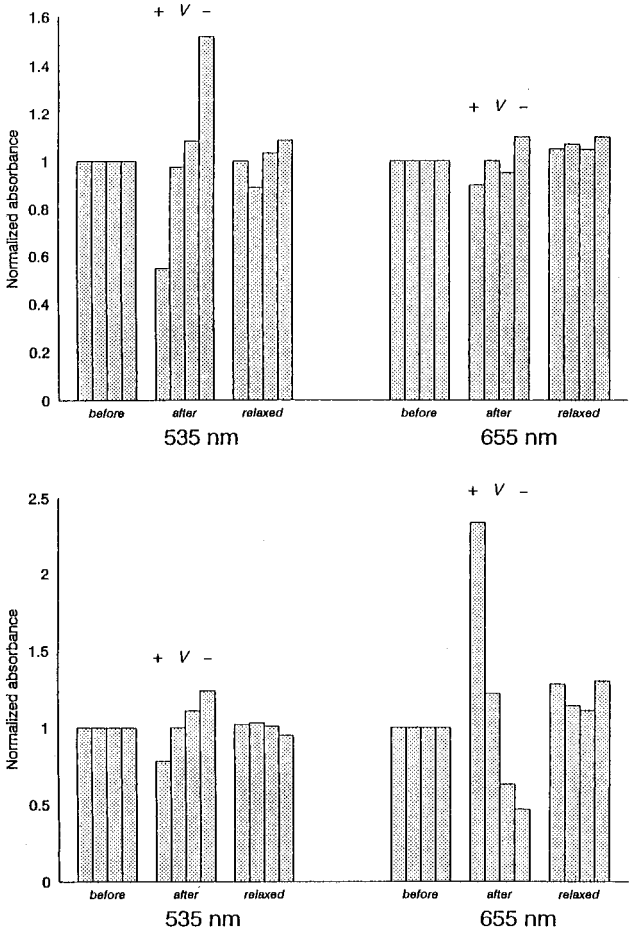

FIGURE 8. (a, top) Optical absorbance of individual membranes (or contiguous stack), immediately before and after an applied potential step, and after an equilibration period (relaxed). This is a constant-resistance membrane nearly fixed site with excess carrier. The red peak is for free carrier; the blue peak is for complexed (in this case) protonated carrier, ETH 5294. Reprinted with permission from ref 58. Copyright 1993 Verlag Helvetica Chimica Acta. (b, bottom) Absorbance of individual membranes (or contiguous stack), immediately before and after a potential step, and after an equilibration period (relaxed). This is a variable-resistance membrane. The red peak is for free carrier; the blue peak is for complexed (in this case) protonated carrier, ETH 5294. Reprinted with permission from ref 58. Copyright 1993 Verlag Helvetica Chimica Acta.

A high-resolution, true imaging technique for studying membrane bulk transport was first described in 1990 by Harrison who determined the concentration profiles of water and metalloporphyrin complexes in sensor membranes using a spatial imaging photometer.[59] The availability of ion-selective chromoionophores has brought about additional possibilities of speciation, and led to the development of high-resolution imaging, spectropotentiometry for visualizing membrane transport phenomena in parallel with the measurement of transient potentials.[60] A membrane ring is mounted in a cell under a microscope. Usually the inner and outer rims of the membrane ring are put in contact with electrolyte solutions. After the system reaches equilibrium a perturbation (activity change, current, or voltage step) is introduced and the relaxation processes leading to a new equilibrium are followed optically and electrochemically. With incorporation of

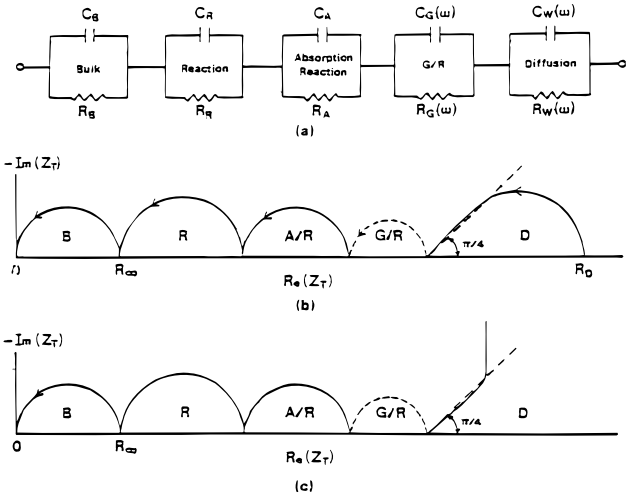

FIGURE 9. Parallel RC elements of electrochemical impedances (a, top) and corresponding impedance plane plots for symmetric (b, middle) and asymmetric cells (c, bottom). Bulk is a high-frequency geometric response. Reaction is the usual slow interfacial kinetics. Absorption/reaction applies to cases with fast (or different) kinetics for surface reactions. G/R is the impedance for generation/recombination which is ion pair formation/dissociation. Diffusion is in the Warburg impedance. Reprinted with permission from ref 55. Copyright 1993 Elsevier.

new lipophilic, water-sensitive dyes, water concentration profiles can be determined as well. By analyzing the profiles, the three pd components of the TMS theory can be fit and thus "determined" under steady-state conditions.

Impedances of Membrane Systems. In addition to optical methods, ac impedance measurements show several features of the TMS theory directly.[3,19,21,27,28,55] The impedance plane plots ($-Z_I$ vs Z_R, imaginary and real impedances) show crucial sensor properties: (1) high-frequency resistance and geometrical capacitance, (2) interfacial kinetics, and (3) diffusion−migration responses at low frequencies for both symmetric and asymmetric cells in Figure 9a. Generally, no more than three features can be resolved from one experimental arrangement. Typical theoretical impedance plane plots for symmetric and asymmetric cells are illustrated in Figure 9b,c. Studies on simple mobile-site systems have shown the value of impedance spectroscopy in understanding the principal features as well as esoteric characteristics of membranes. Examples are dielectric constant dependences on membrane salt content, water uptake by membranes, and second quadrant impedances that occur when lost permselectivity controls one interfacial pd.[12]

Surface Concentration Steps, Chronoamperometry, and I−V Curves. Fixed-site membranes tend to be ohmic and electrically uninteresting. Current−time and current−applied voltage curves for mobile-site membranes, with and without selectivity-enhancing complexing agents, are more interesting. The principal mobile-site examples have shown transport control by site-concentration polarization, or by carrier-concentration polarization.[61−63] In the former case, the current−time curve is Cottrell-like; i.e., current is proportional to $t^{-1/2}$. However, a completely

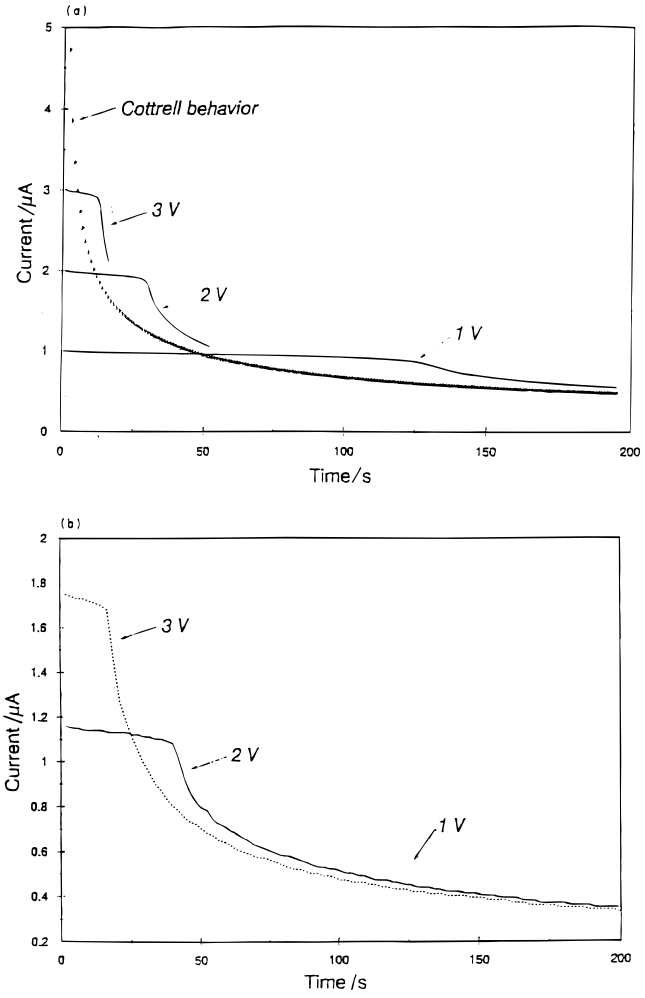

FIGURE 10. (a) Theoretical current vs time responses of plasticized PVC membrane with 1 mM valinomycin (carrier) under various $-V_{applied}$ values. The membrane resistance corresponding to concentration of sites and charged complexes was 10^6 Ω. Thickness 1.0×10^{-4} m; diffusion coefficient of carrier 1.5×10^{-12} m^2 s^{-1}. (b) Experimental results for plasticized PVC membrane with 1 mM valinomycin (carrier) under various $-V_{applied}$ values. This is an example of so-called modified Cottrell behavior. Reprinted with permission from ref 61. Copyright 1992 Elsevier.

new phenomenon occurs when the current is controlled by the carrier-concentration polarization. The chronoamperometric current remains nearly constant (decreases very slowly) at fixed applied voltage until the free carrier concentration is totally concentration polarized. Then, Cottrell-type current decay appears. These experiments have been useful for determining diffusion coefficients of free carrier, ion-bound carrier, and ion−carrier-site complexes for various sensor systems. Examples are illustrated in Figure 10.[63]

Concluding Remarks

A modest selection of achievements in the interpretation or responses of membrane-based electrochemical sensors is presented. The results of classical, thermodynamic-based surface analysis, modern electrochemical impedance spectroscopy, chronoamperometry, and optical methods applied to mobile-site, solvent polymeric, ion-

exchanger-based sensor membranes are summarized. Experimental evaluation of separated interfacial and bulk transport events have shown the validity of the Teorell–Meyer–Sievers model of membrane potentials. Despite the clarity of the results, many passive membrane processes remain to be interpreted and others discovered.

This work was partly supported by the US-Hungarian Joint Fund, JF No. 568, by the NSF-Whitaker Foundation Grant BES-9520526, and by the NSF-ERC Grant CDR-8622201.

References

(1) Buck, R. P. Ion-Transport Phenomena: Charge Exchange and Transport Into and Within "Thick" Ideal Membranes. In *Ion-Transfer Kinetics, Principles and Applications*; Sandifer, J. R., Ed.; VCH Publishers: New York, 1995; Chapter 2, pp 19–54.
(2) Brumleve, T. R.; Buck, R. P. *J. Electroanal. Chem.* **1978**, *90*, 1–31.
(3) Brumleve, T. R.; Buck, R. P. *J. Electroanal. Chem.* **1981**, *126*, 73–104.
(4) Teorell, T. *Proc. Soc. Exp. Biol. Med.* **1935**, *33*, 282.
(5) Teorell, T. *Proc. Soc. Natl. Acad. Sci. U.S.A.* **1935**, *21*, 152.
(6) Meyer, K. H.; Sievers, J. F. *Helv. Chim. Acta* **1936**, *19*, 649, 665, 987.
(7) Buck, R. P.; Vanysek, P. *J. Electroanal. Chem.* **1990**, *292*, 73–91.
(8) Helfferich, F. *Ion Exchange*; McGraw-Hill Book Co: New York, 1962; Chapter 7; pp 323–338.
(9) Buck, R. P.; Stover, F. S.; Mathis, D. E. *J. Electroanal. Chem.* **1977**, *82*, 345–360; **1978**, *94*, 59–66; **1979**, *100*, 63–70.
(10) Buck, R. P.; Toth, K.; Graf, E.; Horvai, G.; Pungor, E. *J. Electroanal. Chem.* **1987**, *223*, 51–66.
(11) Buck, R. P.; Cosofret, V. V.; Lindner, E. *Anal. Chim. Acta* **1993**, *282*, 273–281.
(12) Stover, F. S.; Buck, R. P. *J. Electroanal. Chem.* **1980**, *107*, 165–175.
(13) Buck, R. P. Theory and Principles of Ion Selective Electrodes. In *Ion Selective Electrodes in Analytical Chemistry, Vol. I.;* Freiser, H., Ed.; Plenum Press: New York, 1978, pp 1–141.
(14) Buck, R. P. Electrochemistry of Ion-Selective Electrodes. *Proceedings NATO Advanced Study Institute on Chemically Sensitive Electronic Devices*; (Bergveld, P., Zemel, J., Middelhoek, S., Eds.; Elsevier Publishing Co.: Amsterdam, 1981; pp 197–260.
(15) Buck, R. P. Electrochemistry of Ion-Selective Electrodes. In *Comprehensive Treatise of Electrochemistry Volume 8*; (White, R. E., Bockris, J., Conway, B., Yeager, E., Eds.), Plenum Press: New York, 1984, Chapter 3, p 137–248.
(16) Buck, R. P.; Nahir, T. M.; Cosofret, V. V.; Lindner, E., Erdosy, E. *Anal. Proc. Inc. Anal. Commun.* **1994**, *31*, 304–312.
(17) Lindner, E.; Graf, E.; Niegreisz, Z.; Toth, K.; Pungor, E.; Buck; R. P. *Anal. Chem.* **1978**, *60*, 295–301.
(18) Iglehart, M. L.; Buck, R. P.; Horvai, G.; Pungor, E. *Anal. Chem.* **1988**, *60*, 1018–1022.
(19) Buck, R. P. *J. Electroanal. Chem.* **1986**, *210*, 1–19.
(20) Buck, R. P. *Ann. Biomed. Eng.* **1992**, *20*, 363–383.
(21) Buck, R. P.; Mundt, C. *J. Chem. Soc., Faraday Trans.* **1996**, *92*, 3947–3955.
(22) Buck, R. P. *J. Electroanal. Chem.* **1987**, *219*, 23-.
(23) Buck, R. P. *J. Phys. Chem.* **1988**, *92*, 4196–4200.
(24) Sharp, M. *Anal. Chim. Acta* **1972**, *59*, 137; **1972**, *61*, 99; **1972**, *62*, 385; **1975**, *65*, 405.
(25) Buck, R. P. *J. Membrane Sci.* **1984**, *17*, l-62.
(26) Buck, R. P. Transport Properties of Ionic Conductors. *Proceedings of NATO Advanced Study Institute on Chemically Sensitive Electronic Devices*; (Bergveld, P., Zemel, J., Middelhoek, S., Eds.; Elsevier Publishing Co.: Amsterdam, 1981; pp. 137–196.
(27) Buck, R. P. *Electrochim. Acta* **1990**, *35*, 1609–1617.
(28) Toth, K.; Graf, E.; Horvai, G.; Pungor, E.; Buck, R. P. *Anal. Chem.* **1986**, *58*, 2741–2744.
(29) Sandifer, J. R.; Iglehart, M. L.; Buck, R. P. *Anal. Chem.* **1989**, *61*, 1624–1630.
(30) Iglehart, M. L.; Buck, R. P. *Talanta* **1989**, *36*, 89–98.
(31) Lindner, E.; Niegreisz, Zs.; Toth, K.; Pungor, E, Berube, T. R.; Buck, R. P. *J. Electroanal. Chem.* **1989**, *259*, 67–80.
(32) Parker, A. J. *Chem. Rev.* **1969**, *69*, 1–32.
(33) Vanysek, P. *Electrochemistry on Liquid/Liquid Interfaces, #39 Lecture Notes in Chemistry*; Springer-Verlag: Berlin, 1985.
(34) Reid, J. D.; Melroy, O. W.; Buck, R. P. *J. Electroanal. Chem.* **1983**, *147*, 71–82.
(35) For a recent exposition see: Delahay, P. *Double Layer and Electrode Kinetics*; Wiley-Interscience: New York, 1965; Chapter 2, p 17.
(36) Verwey, E. J. W.; Niessen, K. F. *Philos. Mag.* **1939**, *28*, 435.
(37) Melroy, O. R.; Buck, R. P.; Stover, F. S.; Hughes, H. C. *J. Electroanal. Chem.* **1981**, *121*, 93–114.
(38) Melroy, O. R.; Buck, R. P. *J. Electroanal. Chem.* **1983**, *151*, 1–9.
(39) Benjamin, I. *J. Phys. Chem.* **1991**, *95*, 6675.
(40) Benjamin, I. *J. Phys. Chem.* **1992**, *97*, 1432.
(41) Benjamin, I. *Chem. Rev.* **1996**, *96*, 1449.
(42) Schweighofer, K. J.; Benjamin, I. *J. Electroanal. Chem.* **1995**, *391*, 1.
(43) Melroy, O. R.; Buck, R. P. *J. Electroanal. Chem.* **1982**, *136*, 19–37.
(44) Melroy, O. R.; Buck, R. P. *J. Electroanal. Chem.* **1983**, *143*, 23–36.
(45) Girault, H. H.; Schiffrin, D. J. *J. Electroanal. Chem.* **1983**, *190*, 43.
(46) Girault, H. H. In *Modern Aspects of Electrochemistry*; Bockris, J. O., Conway, E., White, R. E., Eds.; Plenum: New York, 1993; Vol. 25, p 1.
(47) Kakiuchi, T. *J. Electroanal. Chem.* **1992**, *322*, 55.
(48) Kakiuchi, T. *Denki Kagaku* **1993**, *61*, 932.
(49) Kontturi, K.; Manzanares, J. A.; Murtomaki, L. *Electrochim. Acta* **1995**, *40*, 2979.
(50) Senda, M. *Electrochim. Acta* **1995**, *40*, 2993.
(51) Buck, R. P. Crystalline, Pressed Powder, and Supported Solid Membrane Electrodes. In *Ion Selective Electrode Methodology*; Covington, A. K., Ed.; CRC Press: West Palm Beach, FL, 1979; pp 175–250.
(52) Buck, R. P. *J. Electroanal. Chem.* **1989**, *258*, 1–12.
(53) Buck, R. P. *J. Phys. Chem.* **1988**, *92*, 6445–6451.
(54) Buck, R. P. *J. Electroanal. Chem.* **1989**, *271*, 1–14.
(55) Buck, R. P.; Madaras, M. B.; Mäckel, R. *J. Electroanal. Chem.* **1993**, *362*, 33–46.
(56) Franceschetti, D. R.; Macdonald, J. R.; Buck, R. P. *J. Electrochem. Soc.* **1991**, *138*, 1368–1371.
(57) Stover, F. S.; Buck, R. P. *Biophys J.* **1976**, *16*, 753.
(58) Nahir, T. M.; Buck, R. P. *Helvetica Chimica Acta* **1993**, *76*, 407–415.
(59) Li, X.; Petrovic, S.; Harrison, D. J. *Sensors and Actuators* **1990**, *B1*, 275–280.

(60) Schneider, B.; Zwickl, T.; Federer, B.; Pretsch, E.; Lindner, E. *Anal. Chem*. **1996**, *68*, 4342−4350.
(61) Nahir, T. M.; Buck, R. P. *J. Electroanal. Chem*. **1992**, *341*, 1−14.
(62) Nahir, T. M.; Buck, R. P. *Electrochim. Acta* **1993**, *38*, 2691−2697.
(63) Nahir, T. M.; Buck, R. P. *J. Phys. Chem*. **1993**, *97*, 12363−12372.
(64) Reid, J. D.; Vanysek, P.; Buck, R. P. *J. Electroanal. Chem*. **1984**, *161*, 1−15.

AR9700623